

Professional Paper - Chapters 1,2, and 3,
Appendixes A,B
William Cook

0.1 Abstract

Dynamic models that simulate processes across large geographic locations, such as hydrologic models, are often informed by spatially distributed parameters. Spatially distributed parameters are frequently correlated and any techniques utilized in their calibration ideally incorporate existing hierarchical relationships into their structure. In this paper, a parameter estimation method based on the Dual State Ensemble Kalman Filter called the Dual State Hierarchical Ensemble Kalman Filter (DEHnKF) is presented. This modified filter is innovative in that it allows parameters to be placed into a set of groups that are smoothed using hierarchical modeling techniques. The usability and effectiveness of this new technique is demonstrated by applying it to a rainfall-runoff model that simulates subcatchment-scale hydrologic processes and contains high dimensional spatially distributed empirical parameters.

Contents

0.1	Abstract	2
1	Introduction	5
2	The Hierarchical Dual Ensemble Kalman Filter Method	9
2.1	General Dynamic Model and Observations	9
2.2	DEnHKF Method	10
2.2.1	Prediction Phase	10
2.2.2	Parameter Correction Phase	12
2.2.3	State Correction Phase	13
3	Application of DEnHKF to Hydrologic Model	15
3.1	daWUAPhydroengine	15
3.1.1	Input Data	16
3.1.2	Calibrated Parameters	16
3.2	Observation Data	16
3.3	Catchment Data and Hierarchical Groups	17
A	The Dual Ensemble Kalman Filter	21
A.0.1	Prediction Phase	21
A.0.2	Parameter Correction Phase	22
A.0.3	State Correction Phase	23
B	The Hydrologic Model	25
B.0.1	Rainfall Runoff component	25

B.0.2	Routing component	29
-------	-----------------------------	----

Chapter 1

Introduction

Utilizing sequential data assimilation techniques to filter hydrologic models is an efficient way to correct and calibrate them both before and after implementation in the field. Observations such as SWE (snow water equivalent), streamflow, and precipitation are collected on a daily basis across various geographic regions, allowing real time information to be dynamically ingested by the hydrologic model and inform present and future predictions. More accurate models allow hydrologists to better understand the past and predict the future, and the need to research optimal methods of hydrologic data assimilation has been recognized [22] and researched [14], [19]. Observed hydrologic data may allow models, including rainfall-runoff models, to undergo parameter estimation. Parameter estimation for rainfall-runoff models has been a relevant field of research for quite a while [20],[21] and research has progressed into the 21'st century [17], [24].

Models that ingest data sequentially can have their parameters efficiently corrected by a Kalman Filter, a sequential data assimilation algorithm. Kalman Filters only need the previous timestep's state estimate, parameter estimate, and co-variance matrices to update the current timestep's state estimate, parameter estimate, and co-variance matrices. The original Kalman filter[12] was created to solve linear problems and more complicated implementations must be used to solve non-linear problems. The extended Kalman Filter[10] works for mildly non-linear systems but does not function optimally on heavily non-linear systems[16]. The Unscented Kalman

Filter[11] is an all-around improvement on the Extended Kalman Filter that allows for the filtering of highly non-linear systems. The Ensemble Kalman Filter[7], a predecessor to the Unscented Kalman Filter, filters non-linear systems by generating an 'ensemble' of model instances and adding unique noise to each model's forcing data. The main advantage of this ensemble based approach is the substitution of the original Kalman Filter's error covariance matrix with an ensemble covariance matrix, which allows for the efficient computation of the covariance of high dimensional state vectors.

To calibrate model parameters as well as model states a Dual State Kalman Filter may be used as demonstrated by Moradkhani et. al in 2005 [17]. Dual state Kalman filters add a small perturbation to a series of parameters that the user wishes to calibrate. These perturbed parameters vectors are then corrected in a similar fashion to the state vectors. After this happens a second filter is run to correct the state vectors in the traditional fashion. The Dual State Ensemble Kalman Filter implemented by Moradkhani et. al[17] extends the Ensemble Kalman Filter into a dual state configuration and is shown to successfully predict a set of parameters.

An alternative method of parameter estimation that utilizes the Kalman Filter is the Joint Kalman Filter, which combines states and parameters into one vector that is calculated simultaneously without the need for a second run. Joint Ensemble Kalman Filters have been successfully implemented on hydrologic models [23] and other models [5], but Joint Ensemble Kalman filters can suffer from "filter inbreeding" under certain circumstances [9] and introduce inconsistency in especially heterogeneous formations [25]. Overall, Dual Ensemble Kalman Filters are more accurate than Joint Ensemble Kalman Filters, especially in noisy situations, with the major drawback of the Dual approach being its larger draw on computational power [15].

In this paper hierarchical modeling techniques are integrated into the Dual State Ensemble Kalman Filter's parameter perturbation equation to create a Hierarchical Dual State Ensemble Kalman Filter. A hierarchical parameter perturbation framework allows the model to account for parameters that are hierarchically related. To examine the Dual State Hierarchical Ensemble Kalman Filter's application to high

dimensional spatially distributed raster data and geographical data the hydrologic model, a variation of a rainfall-runoff model, is implemented to predict streamflows across the state of Montana. The hydrologic model is informed by a variety of sub-components featuring high dimensional spatially distributed parameters, including a snowpack process, soil process, and a Muskingham-Cunge routing component. Conveniently, these parameters can be linked to individual sub-basins which can in turn be sorted into HUC-4 class watersheds, a situation that favors a hierarchical approach. Despite the model's high-dimensional parameters, the hydrologic model is designed to be a quick and efficient model. Accordingly, a Dual State Hierarchical Ensemble Kalman Filter is an optimal calibration algorithm to calibrate this raster data because 1) the DEHnKF does not have to compute the high dimensional state covariance matrix during the update phase and 2) the hydrologic model is a sequential model that could conceivably benefit from real-time parameter correction.

Chapter 2 covers the methods behind the Dual State Hierarchical Ensemble Kalman Filtering algorithm. Chapter 3 discusses the hydrologic model and how a Dual State Hierarchical Ensemble Kalman Filter was applied to it. Chapter 4 discusses results while Chapter 5 compares those results with calibrated parameters from a Dual State Ensemble Kalman Filter as implemented by Moradkhani et al.

Chapter 2

The Hierarchical Dual Ensemble Kalman Filter Method

2.1 General Dynamic Model and Observations

A generic dynamic model can be defined as one more more discrete nonlinear stochastic processes[5]:

$$x_{t+1} = f(x_t, u_t, \theta_t) + \varepsilon_t \quad (2.1)$$

where x_t is an n dimensional vector representing the state variables of the model at time step t , u_t is a vector of forcing data (e.g temperature or precipitation) at time step t , and θ_t is a vector of model parameters which may or may not change per time step (e.g *soil beta* or *DDF*). The non-linear function f takes these variables as inputs. The noise variable ε_t accounts for both model structural error and for any uncertainty in the forcing data.

A state's observation vector z_t can be defined as

$$z_t = h(x_t, \theta_t) + \delta_t \quad (2.2)$$

Where the x_t vector represents the true state, θ_t represents the true parameters, $h(.)$ is a function that determines the relationship between observation and state

vectors, and δ_t represents observation error. δ_t is Gaussian and independent of ε_t .

The Dual Hierarchical State Ensemble Kalman Filter can be split into three subsections: The prediction phase, the parameter correction phase, and the state correction phase.

2.2 DEnHKF Method

2.2.1 Prediction Phase

Just as in a standard Dual Ensemble Kalman filter (see [Appendix A](#) for the Dual Ensemble Kalman Filter methods as implemented by Moradkhani et al.), each ensemble member i is represented by a stochastic model similar to (2.1). The modified equation is as follows:

$$x_{t+1}^{i-} = f(x_t^{i+}, u_t^i, \theta_t^{i-}) + \omega_t, \quad i = 1, \dots, n \quad (2.3)$$

Where n is the total number of ensembles. The $-/+$ superscripts denote corrected (+) and uncorrected (−) values. Note that θ_t^{i-} 's t subscript does not necessarily denote that θ is time variant but rather indicates that parameter values change as they are filtered over time. The noise term ω_t accounts for model error and will hereafter be excluded from the state equation.

Errors in the model design are accounted for through the perturbation the forcing data vector u_t with random noise ζ_t^i to generate a unique variable u_t^i for each ensemble. ζ_t^i is drawn from a normal distribution with a covariance matrix Q_t^i .

$$u_{t+1}^i = u_t + \zeta_t^i, \quad \zeta_t^i \sim N(0, Q_t^i) \quad (2.4)$$

Legacy Parameter Perturbation

To generate the priori parameters θ_{t+1}^{i-} an evolution of the parameters similar to the evolution of the state variables must be implemented. Legacy implementations of parameter evolution added a small perturbation sampled from $N(0, \Sigma_t^\theta)$, where Σ_t^θ

represents the covariance matrix of θ at timestep t . This legacy method of evolution resulted in overly dispersed parameter samples and the loss of continuity between two consecutive points in time [13] [5]. To overcome this the kernel smoothing technique developed by West [26] and implemented by Liu [13] has been used effectively in previous Dual Ensemble Kalman filter implementations [17] and similar models [5].

$$\theta_{t+1}^{i-} = a\theta_t^{i+} + (1-a)\bar{\theta}_t^+ + \tau_t^i \quad (2.5)$$

$$\tau_t^i = N(0, h^2 V_t) \quad (2.6)$$

Where $\bar{\theta}_t^+$ is the mean of the parameters with respect to the ensembles, $V_t = \text{var}(\theta_t^{i+})$, a is a shrinkage factor between (0,1) of the kernel location, and h is a smoothing factor. h may be defined as $\sqrt{1-a^2}$, while a may fall between (.45,.49) [5]. Note that h and a tend to vary per model and optimal values for these parameters are generally found via experimentation [17] [1] [2] [5].

Hierarchical Parameter Perturbation

In a standard hierarchical linear regression, a value y contained in set of related values $J_g, j = 1, \dots, n$ contained in hierarchical group g can be expressed through the linear equation

$$y_{j,g} = \alpha_g * x + \beta_g, \quad \alpha_g \sim N(\mu_\alpha, \sigma_\alpha), \quad \beta_g \sim N(\mu_\beta, \sigma_\beta) \quad (2.7)$$

where α and β are determined to be hierarchically related properties drawn from their respective normal distributions. For a simple overview of hierarchical models refer to Osborne [18], while [8] is a more in-depth reference.

In a Hierarchical Dual Ensemble Kalman Filter, parameter perturbation has been modified to have properties of a hierarchical linear regressive system. First, ensembles are placed into a series of groups G_g based on shared characteristics (spatial or otherwise.) Algorithms (2.5) and (2.6) are then updated to conform to the hierarchical structure described in (2.7):

$$\theta_{t+1,g}^{i-} = aG_{t,g}^i + (1-a)\bar{\theta}_{t,g}^+ + \tau_{t,g}^i \quad (2.8)$$

$$G_{t,g}^i = N(\mu_\theta, \sigma_\theta) \quad (2.9)$$

$$\tau_t^i = N(0, h^2 V_{t,g}^i) \quad (2.10)$$

Where $\bar{\theta}_{t,g}^{i+}$ is the mean over all ensembles for all members of group g , $G_{t,g}^i$ is a vector of parameters re-sampled from the mean and standard deviation of $\theta_{t+1,g}^{i-}$, and $V_{g,t}$ is the variance matrix with respect to the ensembles of all members of group g .

2.2.2 Parameter Correction Phase

In an Ensemble Kalman Filter, observations are perturbed to reflect model error. To accomplish this n unique perturbations are created. Therefore, the variable z_{t+1}^i is defined as follows:

$$z_{t+1}^i = z_{t+1} + \eta_{t+1}^i, \quad \eta_{t+1}^i = N(0, R_{t+1}) \quad (2.11)$$

Where z_{t+1} is an observation vector defined by (2.2) and η_{t+1}^i is a random perturbation drawn from a normal distribution with covariance matrix R_{t+1} . A set of state predictions that can be related to the observations are generated by running the priori state vector through the function $h(\cdot)$:

$$\hat{y}_{t+1}^i = h(x_{t+1}^{i-}, \theta_{t+1}^{i-}) \quad (2.12)$$

The parameter update equation is similar to the update equation of the linear Kalman filter $\hat{x}_t^+ = \hat{x}_t^- + K_t(z_t - H\hat{x}_t^-)$. Notably, parameters are corrected in lieu of the states:

$$\theta_{t+1}^{i+} = \theta_{t+1}^{i-} + K_{t+1}^\theta(z_{t+1}^i - \hat{y}_{t+1}^i) \quad (2.13)$$

To facilitate this, K_{t+1}^θ is defined as

$$K_{t+1}^\theta = \frac{\Sigma_{t+1}^{\theta, \hat{y}}}{\Sigma_{t+1}^{\hat{y}, \hat{y}} + R_{t+1}} \quad (2.14)$$

where $\Sigma_{t+1}^{\theta, \hat{y}}$ is the cross covariance of θ_{t+1} and \hat{y}_{t+1} , $\Sigma_{t+1}^{\hat{y}, \hat{y}}$ is the covariance of \hat{y}_{t+1} , and R_{t+1} is the observation error matrix from (2.11).

2.2.3 State Correction Phase

After θ_{t+1}^{i+} has been calculated the model is run again (2.3) with the θ_{t+1}^{i+} replacing θ_{t+1}^{i-} .

$$x_{t+1}^{i-} = f(x_t^{i+}, u_t^i, \theta_t^{i+}), \quad i = 1, \dots, n \quad (2.15)$$

After a new state vector is generated it is re-run through (2.12) with the new parameter vector:

$$\hat{y}_{t+1}^i = h(x_{t+1}^{i-}, \theta_{t+1}^{i+}) \quad (2.16)$$

The corrected state vector is then run through the state update equation

$$x_{t+1}^{i+} = x_{t+1}^{i-} + K_{t+1}^x (z_{t+1}^i - \hat{y}_{t+1}^i) \quad (2.17)$$

$$K_{t+1}^x = \frac{\Sigma_{t+1}^{x, \hat{y}}}{\Sigma_{t+1}^{\hat{y}, \hat{y}} + R_{t+1}} \quad (2.18)$$

where $\Sigma_{t+1}^{x, \hat{y}}$ is the cross covariance of x_{t+1} and \hat{y}_{t+1} .

Chapter 3

Application of DEnHKF to Hydrologic Model

3.1 daWUAHydroengine

The hydrologic model is used to test the viability of the DEnHKF method. The hydrologic model takes streamflow parameters, subbasin parameters, precipitation, minimum temperatures, and maximum temperatures as inputs and outputs streamflow data along with some additional states such as snow water equivalent. The hydrologic model was designed to be implemented in any geographic location. For this study it was utilized to model streamflows throughout the state of Montana.

For the purposes of this study configuring the hydrologic model to model streamflows throughout Montana is advantageous because it allows for the calibration of a very large number of spatially distributed, high dimensional parameters. These parameters can be expected to vary significantly across the entirety of Montana, a state which covers an area of $380,800 \text{ km}^2$, sports diverse terrain, and is comprised

Table 3.1: States

State (x)	Purpose	Dimensions
streamflow	Streamflow (in cumecs)	330
swe	Snow Water Equivalent (in mm^3)	45012

Table 3.2: Forcing Data

Forcing Data (u)	Purpose	Dimensions
tempmin	Lowest temperature for timestep	45012
tempmax	Highest temperature for timestep	45012
precipitation	Amount of rainfall for timestep	45012

of 3 HUC4 zones.

3.1.1 Input Data

The hydrologic model takes rasterized precipitation data and temperature data from meteorological databases as input. This data can be utilized as forcing data in the ensemble kalman filter framework.

3.1.2 Calibrated Parameters

The hydrologic model utilizes a HBV rainfall-runoff component and a Muskingum-Cunge routing component. The HBV component includes a precipitation and snow-pack process that utilizes the empirical parameter ddf (degree day factor), a soil process that utilizes the empirical parameters aet_lp , $soil_beta$, and $soil_max_wat$ (evapo-transpiration, immediate runoff, and topsoil storage capacity), and a runoff generation process that utilizes the empirical parameters $ck0$, $ck1$, $ck2$, $hl1$, and $perc$, all of which control various aspects of groundwater percolation and runoff. The Muskingum-Cunge routing component utilizes e and K , which control wave dispersion and wave celerity respectively. To learn more about the hydrologic model, its algorithms, and the parameters that control it refer to [Appendix B](#).

3.2 Observation Data

A Kalman Filter relies on one or more observed states for correction. Accordingly, observations were obtained for streamflows across Montana and snowfall across Montana. For streamflow, USGS streamflow data was collected at 86 sites. Each observed site was paired with the closest simulated stream outlet within a 2.5 mile cutoff. For

Table 3.3: Calibrated Parameters

Parameter (θ)	Purpose	Dimensions
<i>ddf</i>	Degree Day Factor	331
<i>aet_lp</i>	Potential Evapo-Transpiration	331
<i>soil_beta</i>	Portion of ponded water that goes into soil storage	331
<i>soil_max_wat</i>	Soil compartment maximum water capacity	331
<i>ck0</i>	Immediate runoff	330
<i>ck1</i>	Fast runoff	330
<i>ck2</i>	Groundwater runoff	330
<i>hl1</i>	Groundwater water storage threshold	330
<i>perc</i>	Groundwater percolation	330
<i>K</i>	Wave celerity	330
<i>e</i>	Wave dispersion	330

Table 3.4: Observations

Observed State (x)	Source	Dimensions
streamflow	USGS	82
swe	NRCS	90

snowfall, SNOWTEL sites monitored by the Natural Resources Conservation Service (NRCS) were used 3-1. 90 stations were chosen and matched to specific pixels in the hydrologic model’s raster files.

3.3 Catchment Data and Hierarchical Groups

The hydrologic model uses HUC8 data to separate Montana into 330 watersheds 3-2. Each watershed is associated with one of each type of parameter from Table 3.3. These 330 watersheds fall into 3 larger HUC4 zones that were utilized to classify each watershed into one of 3 hierarchical zones 3-3.

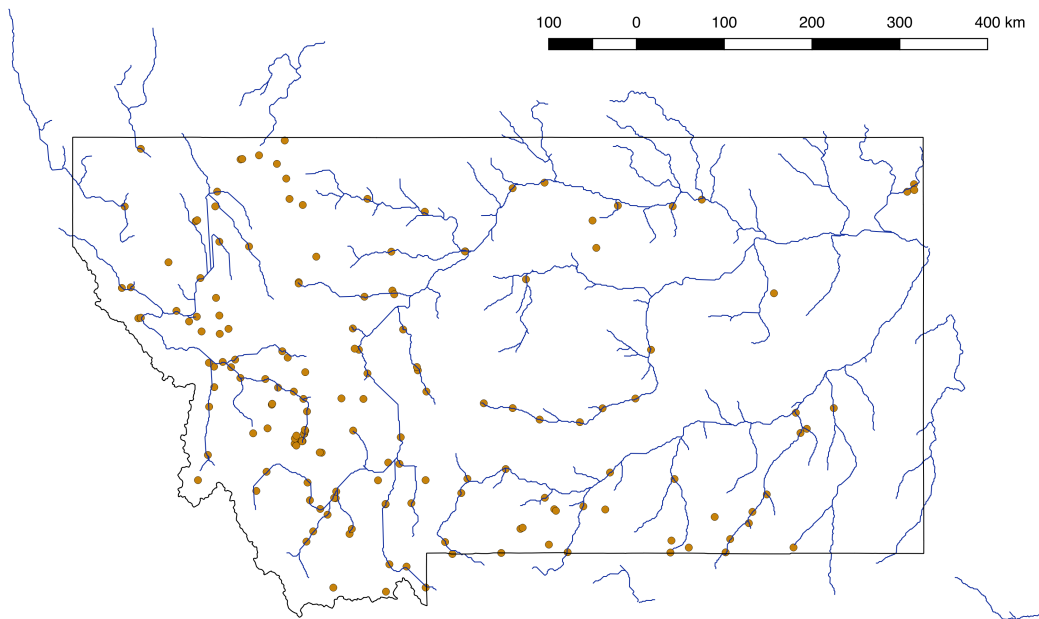


Figure 3-1: all SWE stations plotted against modeled streamflows

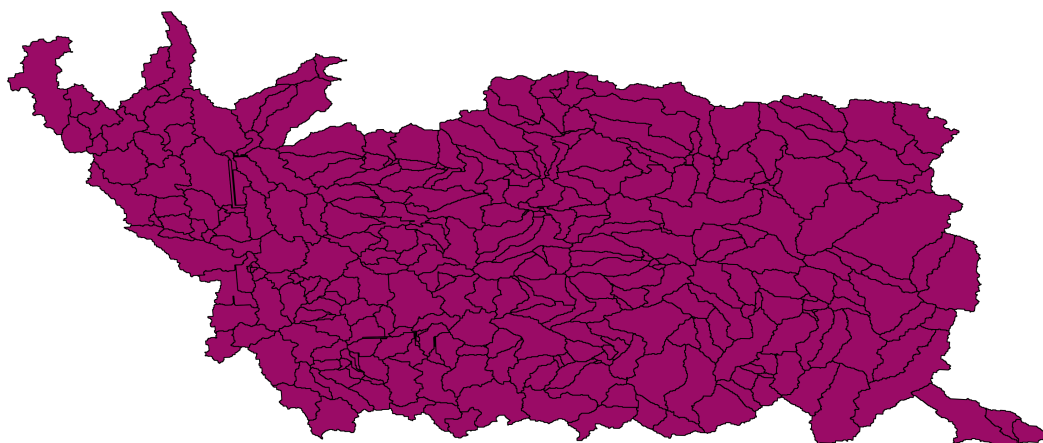


Figure 3-2: Subbasins - HUC8 polygons

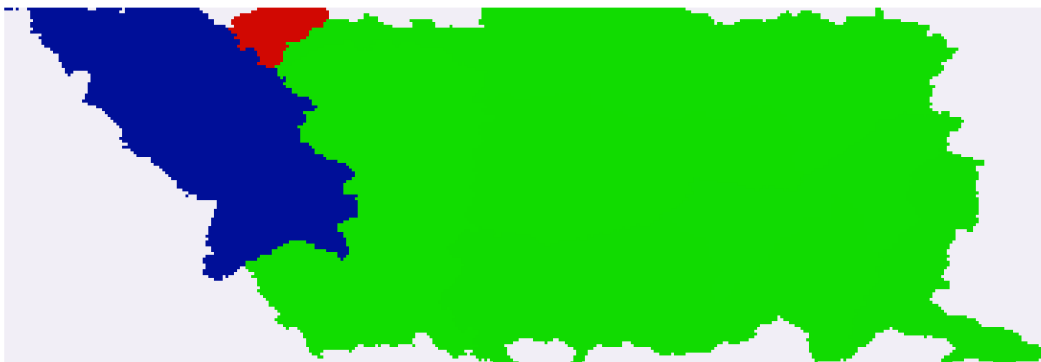


Figure 3-3: Montana's 3 HUC4 zones rendered onto the raster grid.

Appendix A

The Dual Ensemble Kalman Filter

A.0.1 Prediction Phase

In a Dual Ensemble Kalman filter, each ensemble member i is represented by a stochastic model similar to (2.1). The modified equation is as follows:

$$x_{t+1}^{i-} = f(x_t^{i+}, u_t^i, \theta_t^{i-}) + \omega_t, \quad i = 1, \dots, n \quad (\text{A.1})$$

Where n is the total number of ensembles. The $-/+$ superscripts denote corrected (+) and uncorrected (−) values. Note that θ_t^{i-} 's t superscript does not necessarily denote that θ is time variant but rather indicates that parameter values change as they are filtered over time. The noise term ω_t accounts for model error and will hereafter be excluded from the state equation.

Errors in the forcing data are accounted for through the perturbation the forcing data vector u_t with random noise ζ_t^i to generate a unique variable u_t^i for each ensemble. ζ_t^i is drawn from a normal distribution with a covariance matrix Q_t^i .

$$u_{t+1}^i = u_t + \zeta_t^i, \quad \zeta_t^i \sim N(0, Q_t^i) \quad (\text{A.2})$$

To generate the priori parameters θ_{t+1}^{i-} an evolution of the parameters similar to the evolution of the state variables must be implemented. To accomplish this the kernel smoothing technique developed by West [26] and implemented by Liu [13] is

used. Legacy implementations of parameter evolution added a small perturbation sampled from $N(0, \Sigma_t^\theta)$, where Σ_t^θ represents the covariance matrix of θ at timestep t . This legacy method of evolution resulted in overly disposed parameter samples and the loss of continuity between two consecutive points in time [13] [5]. Kernel smoothing has been used effectively to solve this problem in previous Dual Ensemble Kalman filter implementations [17] and similar models [5].

$$\theta_{t+1}^{i-} = a\theta_t^{i+} + (1-a)\bar{\theta}_t^+ + \tau_t^i \quad (\text{A.3})$$

$$\tau_t^i = N(0, h^2 V_t) \quad (\text{A.4})$$

Where $\bar{\theta}_t^+$ is the mean of the parameters with respect to the ensembles, $V_t = \text{var}(\theta_t^{i+})$, a is a shrinkage factor between (0,1) of the kernel location, and h is a smoothing factor. h is defined by $\sqrt{1-a}/2$, while a is generally between (.45,.49). Note that h and a tend to vary per model and optimal values for these parameters are generally found via experimentation [17] [1] [2] [5].

A.0.2 Parameter Correction Phase

In an Ensemble Kalman Filter, observations are perturbed to reflect model error. Therefore, the variable z_{t+1}^i is defined as follows:

$$z_{t+1}^i = z_{t+1} + \eta_{t+1}^i, \quad \eta_{t+1}^i = N(0, R_{t+1}) \quad (\text{A.5})$$

Where z_{t+1} is an observation vector defined by (2.2) and η_{t+1}^i is a random perturbation drawn from a normal distribution with covariance matrix R_{t+1} . A set of state predictions that can be related to the observations are generated by running the priori state vector through the function $h(\cdot)$:

$$\hat{y}_{t+1}^i = h(x_{t+1}^{i-}, \theta_{t+1}^{i-}) \quad (\text{A.6})$$

The parameter update equation is similar to the update equation of the linear Kalman filter $\hat{x}_t^+ = \hat{x}_t^- + K_t(z_t - H\hat{x}_t^-)$. Notably, parameters are corrected in lieu of

the states:

$$\theta_{t+1}^{i+} = \theta_{t+1}^{i-} + K_{t+1}^{\theta} (z_{t+1}^i - \hat{y}_{t+1}^i) \quad (\text{A.7})$$

To facilitate this, K_{t+1}^{θ} is defined as

$$K_{t+1}^{\theta} = \frac{\Sigma_{t+1}^{\theta, \hat{y}}}{\Sigma_{t+1}^{\hat{y}, \hat{y}} + R_{t+1}} \quad (\text{A.8})$$

where $\Sigma_{t+1}^{\theta, \hat{y}}$ is the cross covariance of θ_{t+1} and \hat{y}_{t+1} , $\Sigma_{t+1}^{\hat{y}, \hat{y}}$ is the covariance of \hat{y}_{t+1} , and R_{t+1} is the observation error matrix from (A.5).

A.0.3 State Correction Phase

After θ_{t+1}^{i+} has been calculated the model is run again (A.1) with the θ_{t+1}^{i+} replacing θ_{t+1}^{i-} .

$$x_{t+1}^{i-} = f(x_t^{i+}, u_t^i, \theta_t^{i+}), \quad i = 1, \dots, n \quad (\text{A.9})$$

After a new state vector is generated it is re-run through (A.6) with the new parameter vector:

$$\hat{y}_{t+1}^i = h(x_{t+1}^{i-}, \theta_{t+1}^{i+}) \quad (\text{A.10})$$

The corrected state vector is then run through the state update equation

$$x_{t+1}^{i+} = x_{t+1}^{i-} + K_{t+1}^x (z_{t+1}^i - \hat{y}_{t+1}^i) \quad (\text{A.11})$$

$$K_{t+1}^x = \frac{\Sigma_{t+1}^{x, \hat{y}}}{\Sigma_{t+1}^{\hat{y}, \hat{y}} + R_{t+1}} \quad (\text{A.12})$$

where $\Sigma_{t+1}^{x, \hat{y}}$ is the cross covariance of x_{t+1} and \hat{y}_{t+1} .

Appendix B

The Hydrologic Model

The hydrologic model is a hydrologic system that couples a rainfall-runoff model to a routing component that simulates streamflows inside a regional stream network. An HBV model [3, 4] was modified to simulate hydrologic processes like snowmelt, evapotranspiration, and infiltration at the subcatchment level and transform the resulting precipitation into runoff and streamflow. This streamflow is then routed via the Muskingum-Cunge routing algorithm [6]. Below is a description of the implementation of those algorithms.

B.0.1 Rainfall Runoff component

The HBV model [3, 4] contains a mixture of raster-based and vector-based operations. Raster-based operations utilize spatially distributed data drawn from meteorological databases (precipitation and temperature data.) The raster grid is also used to calculate snow accumulation, melt, and soil processes. These are informed both by input from the meteorological databases and by a series of spatially distributed parameters, such as potential evapotranspiration. Vector-based operations increase computational efficiency through the use of polygons. Uniform hydrologic response units (HRUs) are implemented to aggregate runoff production over these polygons.

Precipitation and snowpack processes To determine the amount of precipitation that becomes snowfall and which amount becomes rainfall, minimum and

maximum temperature data are compared to a critical temperature threshold Tc .

$$Snow_j^t = \begin{cases} P_j^t & T_{max_j^t} < Tc_j \\ P_j^t * \frac{Tc_j - T_{min_j^t}}{T_{max_j^t} - T_{min_j^t}} & T_{min_j^t} < Tc_j < T_{max_j^t} \\ 0 & T_{min_j^t} > Tc_j \end{cases} \quad (B.1)$$

$$Rain_j^t = P_j^t - Snow_j^t \quad (B.2)$$

Where variables and parameters with a subscript j are spatially distributed and are at gridpoint j and variables and parameters with a superscript t are time-dynamic. P is precipitation (mm d^{-1}), T_{max} is maximum air temperature, T_{min} is minimum air temperature ($^{\circ}\text{C}$), $Rain$ is liquid precipitation and $Snow$ is snowfall (mm d^{-1}). Any snowfall during one day t contributes to the snowpack's snow water equivalent (SWE , (mm)):

$$SWE_i^t = SWE_i^{t-1} + Snow_j^t \Delta t \quad (B.3)$$

A degree day model is utilized to simulate snowpack melt. Snowpack begins to melt when the average air temperature exceeds air temperature threshold Tm .

$$Melt_j^t = ddf_j * (Tav_j^t - Tm_j) \text{ for } Tav_j^t > Tm_j \quad (B.4)$$

$$Rain_j^t = P_j^t - Snow_j^t \quad (B.5)$$

Where $Melt$ represents water released from the snowpack (mm d^{-1}), Tav is average air temperature over the time step ($^{\circ}\text{C}$), and ddf is the degree day factor ($\text{mm d}^{-1} ^{\circ}\text{C}^{-1}$). ddf is an empirical parameter controlling the snowmelt rate per degree of air temperature above temperature threshold Tm .

Melt from the snowpack at time t is subtracted from the snowpack and added to the amount of ponded water:

$$Pond_j^t = Pond_j^{t-1} + (Melt_j^t + Rain_j^t)\Delta t \quad (\text{B.6})$$

$$SWE_j^t = SWE_j^t - Melt_j^t \Delta t \quad (\text{B.7})$$

Where $Pond$ (mm) represents liquid water ponding at the surface.

Soil processes Pondered water either infiltrates into the soil and is either placed in the soil system or is added to the topsoil compartment where it generates speedy runoff. The fraction of ponded water that infiltrates is an exponential function of the relative water storage already in the soil:

$$\Delta SM_j^t = Pond_j^t * \left(1 - \frac{SM_j^t}{FC_j^t}\right)^\beta \quad (\text{B.8})$$

$$(\text{B.9})$$

where SM (mm) is the amount of water in the soil compartment and FC (mm) is the maximum capacity of water the soil compartment can hold before water begins percolating to the groundwater system. β (dimensionless) is an empirical parameter. Actual evapotranspiration (AET , mm d^{-1}) is calculated at the same time. Actual evapotranspiration reduces the amount of water storage in the soil and, just like ΔSM_j^t , is informed by the degree of saturation in the soil (SM over FC).

$$AET_j^t = PET_j^t * \left(\frac{SM_j^t}{FC_j * LP_j}\right)^l \quad (\text{B.10})$$

$$(\text{B.11})$$

where PET is potential evapotranspiration (mm d^{-1}) and l (dimensionless) is an empirical parameter. Soil water storage dynamics and the amount of surface water that generates fast runoff are controlled by infiltration and actual evapotranspiration:

$$SM_j^t = SM_j^{t-1} + \Delta SM_j^t - AET_j^t \Delta t \quad (\text{B.12})$$

$$OVL_j^t = Pond_j^t - \Delta SM_j^t \quad (\text{B.13})$$

where OVL (mm) represents water that recharges the near-surface runoff-generating compartment.

Groundwater Compartments and runoff generation The groundwater system is comprised of two ground-water compartments that generate outflow. The top compartment's outflow represents both immediate runoff and fast runoff. The lower compartment's outflow represents baseflow. These processes are performed at the HRU level, which means that overland flow and soil moisture values, both of which are represented over the raster grid, are averaged over overlaid polygonal subwatersheds representing HRUs. Spatial arithmetic that averages soil water storage over all grid cells j contained within a given polygonal HRU k is indicated by angle brackets $\langle . \rangle$. The mass balance and percolation of water from the upper to the lower compartment of the groundwater system is implemented as:

$$Rech_k^t = \langle OVL_j^t \rangle_k + \langle \max(SM_j^t - FC_j, 0) \rangle_k \quad (\text{B.14})$$

$$SUZ_k^t = SUZ_k^{t-1} + Rech_k^t + Pond_k^t - Q0_k^t \Delta t - Q1_k \Delta t - PERC_k \quad (\text{B.15})$$

$$SLZ_k^t = SLZ_k^{t-1} + PERC_k - Q2 \Delta t \quad (\text{B.16})$$

$Rech$ (mm) represents water storage in the fast runoff generating near-surface compartment, SUZ (mm) represents the storage in the upper groundwater compartment, and SLZ (mm) represents water storage in the lower groundwater compartment in HRU k at time step t . $Q0$, $Q1$, and $Q2$ (mm d^{-1}) are each unique runoff rates. $Q0$ represents the soil surface runoff rate, $Q1$ represents the upper soil compartment runoff rate, and $Q2$ lower soil compartment runoff rate. These are calculated as follows:

$$Q0_k^t = \max((SUZ_k - HL1_k) * \frac{1}{CK0_k}, 0.0) \quad (\text{B.17})$$

$$Q1_k^t = SUZ_k * \frac{1}{CK1_k} \quad (\text{B.18})$$

$$Q2_k^t = SLZ_k * \frac{1}{CK2_k} \quad (\text{B.19})$$

$$Qall_k^t = Q0_k^t + Q1_k^t + Q2_k^t \quad (\text{B.20})$$

$HL1$ (mm) is an empirical parameter controlling a water storage threshold that triggers the generation of fast runoff. $CK0$, $CK1$, and $CK2$ (d) are empirical parameters that represent the characteristic drainage times of the soil surface, upper compartment, and lower compartment respectively.

Total outflow from any given HRU k on day t is distributed over time in order to produce the catchment response. This is accomplished through the convolution the output of HRU k by triangular standard unit hydrograph with base M_{base} .

$$Q_j^t = \sum_{i=1}^{M_{base}} Qall_j^{t-i+1} U(i) \quad (\text{B.21})$$

$$U(i) = \begin{cases} \frac{4}{M_{base}^2} * i & 0 < i < M_{base}/2 \\ -\frac{4}{M_{base}^2} * i + \frac{4}{M_{base}} & M_{base}/2 < i < M_{base} \end{cases} \quad (\text{B.22})$$

where U is a triangular hydrograph of area 1 and a base integer $MAXBAS$ (d) representing the duration of the hydrograph.

B.0.2 Routing component

The runoff responses generated from each HRU are routed through the stream network via the Muskingum-Cunge routing model. Each stream reach k has a storage given by the proceeding discharge-storage equation.

$$S_k^t = K [eQ_{in} + (1 - e)Q_{out}], \quad (\text{B.23})$$

where K (d) and e (dimensionless) are empirical parameters controlling the celerity and dispersion of the wave routed through the channel respectively.

Substituting this relationship in a finite-difference form of the continuity equation $\frac{S_j^{t+1} - S_j^t}{\Delta t} = Q_{in} - Q_{out}$ for a multi-reach system with lateral inflows injected to the upstream of reach dreaming *HRU* j at an average constant rate through timestep t q_j^{t+1} results in:

$$Q_j^{t+1} [K_j(1 - e_j) + 0.5\Delta t] + Q_{j-1}^{t+1} [K_j e_j - 0.5\Delta t] \quad (\text{B.24})$$

$$= Q_j^t [K_j(1 - e_j) - 0.5\Delta t] + Q_{j-1}^t [K_j e_j + 0.5\Delta t] \quad (\text{B.25})$$

$$+ q_j^{t+1} [K_j(1 - e_j) + 0.5\Delta t] \quad (\text{B.26})$$

Each *HRU* contains one reach with an upstream and a downstream node. Stream-flow reaches $j = 1, \dots, J$ are integrated with respect to time using a first-order explicit finite difference scheme. The system of J equations can be assembled as a linear system of the form:

$$\mathbf{A}\mathbf{Q}^{t+1} = \mathbf{B} \quad (\text{B.27})$$

\mathbf{Q}^{t+1} is a vector of unknown streamflows at time $t + 1$ solved each time step for every reach in J . The matrices \mathbf{A} and \mathbf{B} are functions of the model parameters and streamflows at t :

$$\mathbf{A} \equiv (\mathbf{a} + \Phi \mathbf{b})^T \quad (\text{B.28})$$

$$\mathbf{B} \equiv (\mathbf{d} + \Phi \mathbf{c})^T \mathbf{Q}^t + \mathbf{I}(\mathbf{a} \odot \mathbf{q}^{t+1}) \quad (\text{B.29})$$

where Φ is a $J \times J$ sparse connectivity (0,1)-matrix defining which pairs of nodes are connected. Flow direction is from row nodes to column nodes. All rows representing upstream nodes of *HRUs* that drain an outlet node are zeros. Lastly:

$$\mathbf{a} = \mathbf{I}(\mathbf{K} - \mathbf{K} \odot \mathbf{e}) + dt * 0.5 \quad (\text{B.30})$$

$$\mathbf{b} = \mathbf{I}(\mathbf{K} \odot \mathbf{e}) - dt * 0.5 \quad (\text{B.31})$$

$$\mathbf{c} = \mathbf{I}(\mathbf{K} - \mathbf{K} \odot \mathbf{e}) - dt * 0.5 \quad (\text{B.32})$$

$$\mathbf{d} = \mathbf{I}(\mathbf{K} \odot \mathbf{e}) + dt * 0.5 \quad (\text{B.33})$$

\mathbf{K} is an identity matrix of order J . e and \mathbf{K} are column vectors holding parameters e and K for every reach in N . The \odot operator denotes the Schur (elementwise) product between two vectors. The solution of (B.27) will become unstable if $\Delta t > 2 * K_j * (1 - e_j)$. To guard against this an adaptive time stepping scheme was implemented. In this adaptive scheme the default timestep is reduced by an integer fraction until the stability condition is satisfied for all reaches.

Bibliography

- [1] Jeffrey L. Anderson, Stephen L. Anderson, Jeffrey L. Anderson, and Stephen L. Anderson. A Monte Carlo Implementation of the Nonlinear Filtering Problem to Produce Ensemble Assimilations and Forecasts. *Monthly Weather Review*, 127(12):2741–2758, dec 1999.
- [2] J. D. Annan, D. J. Lunt, J. C. Hargreaves, and P. J. Valdes. Parameter estimation in an atmospheric GCM using the Ensemble Kalman Filter. *Nonlinear Processes in Geophysics*, 12(3):363–371, feb 2005.
- [3] S. Bergström. The HBV model - its structure and applications. *Swedish Meteorological and Hydrological Institute Reports Hydrology*, 1992.
- [4] Sten Bergström. Development and Application of a Conceptual Runoff Model for Scandinavian Catchments. *Smhi*, 1976.
- [5] M. Chen, S. Liu, L.L. Tieszen, and D.Y. Hollinger. An improved state-parameter analysis of ecosystem models using data assimilation. *Ecological Modelling*, 219(3-4):317–326, dec 2008.
- [6] L.W Mays V.T Chow D.R Maidment. Unit Hydrograph. In *Applied Hydrology*. McGraw-Hill, New York, 1988.
- [7] Geir Evensen. Sequential data assimilation with a nonlinear quasi-geostrophic model using Monte Carlo methods to forecast error statistics. *Journal of Geophysical Research*, 99(C5):10143, may 1994.
- [8] Andrew Gelman, John B. Carlin, Hal S. Stern, David B. Dunson, Aki Vehtari, Donald B. Rubin, John B. Carlin, Hal S. Stern, David B. Dunson, Aki Vehtari, and Donald B. Rubin. *Bayesian Data Analysis, Third Edition*. Chapman and Hall/CRC, nov 2018.
- [9] H. J. Hendricks Franssen and W. Kinzelbach. Real-time groundwater flow modeling with the Ensemble Kalman Filter: Joint estimation of states and parameters and the filter inbreeding problem. *Water Resources Research*, 44(9), sep 2008.
- [10] Andrew H. Jazwinski. Stochastic Processes and Filtering. *Mathematics in Science and Engineering*, 1970.

- [11] Simon J. Julier and Jeffrey K. Uhlmann. New extension of the Kalman filter to nonlinear systems. volume 3068, page 182. International Society for Optics and Photonics, jul 1997.
- [12] R. E. Kalman. A New Approach to Linear Filtering and Prediction Problems. *Journal of Basic Engineering*, 82(1):35, mar 1960.
- [13] Fang Liu and Fang Liu. Bayesian Time Series: Analysis Methods Using Simulation-Based Computation. 2000.
- [14] Yuqiong Liu and Hoshin V. Gupta. Uncertainty in hydrologic modeling: Toward an integrated data assimilation framework. *Water Resources Research*, 43(7), jul 2007.
- [15] Stefano Mariani and Alberto Corigliano. Impact induced composite delamination: state and parameter identification via joint and dual extended Kalman filters. *Computer Methods in Applied Mechanics and Engineering*, 194(50-52):5242–5272, dec 2005.
- [16] Robert N. Miller, Michael Ghil, and François Gauthiez. Advanced Data Assimilation in Strongly Nonlinear Dynamical Systems. *Journal of the Atmospheric Sciences*, 51(8):1037–1056, apr 1994.
- [17] Hamid Moradkhani, Soroosh Sorooshian, Hoshin V. Gupta, and Paul R. Houser. Dual state-parameter estimation of hydrological models using ensemble Kalman filter. *Advances in Water Resources*, 28(2):135–147, feb 2005.
- [18] Jason W. Osborne. Advantages of hierarchical linear modeling. Osborne, Jason W. *Research & Evaluation*, 7(1), 2000.
- [19] Rolf H. Reichle. Data assimilation methods in the Earth sciences. *Advances in Water Resources*, 31(11):1411–1418, nov 2008.
- [20] Soroosh Sorooshian and John A. Dracup. Stochastic parameter estimation procedures for hydrologic rainfall-runoff models: Correlated and heteroscedastic error cases. *Water Resources Research*, 16(2):430–442, apr 1980.
- [21] Soroosh Sorooshian, Qingyun Duan, and Vijai Kumar Gupta. Calibration of rainfall–runoff models: Application of global optimization to the Sacramento Soil Moisture Accounting Model. *Water Resources Research*, 29(4):1185–1194, apr 1993.
- [22] Peter A. Troch, Claudio Paniconi, and Dennis McLaughlin. Catchment-scale hydrological modeling and data assimilation. *Advances in Water Resources*, 26(2):131–135, feb 2003.
- [23] Jasper A. Vrugt, Cees G. H. Diks, Hoshin V. Gupta, Willem Bouten, and Jacobus M. Verstraten. Improved treatment of uncertainty in hydrologic modeling: Combining the strengths of global optimization and data assimilation. *Water Resources Research*, 41(1), jan 2005.

- [24] Thorsten Wagener and Howard S. Wheater. Parameter estimation and regionalization for continuous rainfall-runoff models including uncertainty. *Journal of Hydrology*, 320(1-2):132–154, mar 2006.
- [25] Xian-Huan Wen and Wen H. Chen. Real-Time Reservoir Model Updating Using Ensemble Kalman Filter With Confirming Option. *SPE Journal*, 11(04):431–442, dec 2006.
- [26] Mike West. Mixture models, Monte Carlo, Bayesian updating, and dynamic models. *Computing Science and Statistics*, 1993.